Microelectronics Journal ∎ (∎∎∎∎) ∎∎∎–∎∎∎

Contents lists available at ScienceDirect

Microelectronics Journal

journal homepage: www.elsevier.com/locate/mejo

Minimizing thermally induced interfacial shearing stress in a thermoelectric module with low fractional area coverage

Amirkoushyar Ziabari [a], Ephraim Suhir [b], Ali Shakouri [a,*]

[a] Birck Nanotechnology Center, Department of Electrical and Computer Engineering, Purdue University, West Lafayette, IN 47907, USA
[b] Department of Mechanical and Materials Engineering, Portland State University, Portland, OR, USA

ARTICLE INFO

Article history:
Received 1 December 2012
Received in revised form
25 October 2013
Accepted 16 December 2013

Keywords:
Thermo-electric module
Interfacial stress
Thermal stress
Analytical modeling
Finite element method

ABSTRACT

High temperature differences between the ceramic parts in thermo-electric modules (TEMs) intended for high temperature applications makes the TEMs vulnerable to the elevated thermal stress leading to possible structural (mechanical) failures. The problem of reducing the interfacial shearing stress in a TEM structure is addressed using analytical and finite-element-analysis (FEA) modeling. The maximum shearing stress occurring at the ends of the peripheral legs (and supposedly responsible for the structural robustness of the assembly) is calculated for different leg sizes. Good agreement between the analytical and FEA predictions has been found. It is concluded that the shearing stress can be effectively reduced by using thinner (smaller fractional area coverage) and longer (in the through thickness direction of the module) legs and compliant interfacial materials.

1. Introduction

Thermo-electric modules (TEMs) have recently received increased attention in connection with the development of advanced energy technologies [1,2]. Extensive research is being conducted in integrating thermo-electric devices into microelectronic ICs for the purposes of both cooling and pumping heat. On-chip solid-state cooling has been addressed by many researchers. Thin film thermoelectric micro-coolers might exhibit high cooling capability [3,4], provide highly localized cooling and temperature stabilization and could be effectively integrated into Si-based microelectronic systems. Nano-structured Bi_2–Te_3-based thin-film thermoelectric coolers could be integrated into state-of-the-art electronic packages [5]. MEMS-based thermoelectric devices [6] are also an attractive and possible alternative to solve many thermal management related problems in microelectronics. Improving material properties in order to enhance the power factor and the thermoelectric figures of merit are important areas of interest [7,8]. Although finding an optimal TEM design and the adequate materials is important to maximize the efficiency of TEMs, the mechanical stability and reliability of the TEMs is equally important. For instance, in the case of thermo-electric coolers in CPU cooling applications, while the designers concentrate on improving the functional performance of the TEM designs, the reliability of TEMs is also a major concern: their mechanical failure would cause overheating and significant reduction in the CPU lifetime [9].

Elevated thermal stresses are viewed today as major bottle-necks for reliability and robustness of high temperature TEM technologies. These stresses are caused, first of all, by the significant differences in temperature between the “hot” and the “cold” ceramic plates in a TEM design (Fig. 1). The thermal stress problem can be solved by selecting adequate thermoelectric materials [10,11] as well as by finding effective ways to reduce the stress level [12].

In this study an analytical and a finite-element-analysis (FEA) models are used to evaluate the thermal stresses in a simplified (two-leg) TEM design. State-of-the-art finite element modeling software, ANSYS [13], is used with an objective to validate the previously suggested analytical model [12]. The obtained information is intended to be helpful as a useful guide when creating a mechanically robust TEM design.

The rest of this paper is organized as follows. The analytical model is described in Section 2. In Section 3, we have employed the model to calculate the shearing stress in different TEM designs. Discussion of the results and comparison with FEM data are also presented. The paper concludes in Section 4 with a summary and possible future work.

2. Analytical modeling

2.1. Assumptions

The following major assumptions are used in the analysis:

- All the materials behave in the elastic fashion.
- Instead of addressing the actual three-dimensional TEM structure, a two-dimensional longitudinal cross-section of this

* Corresponding author. Tel.: +1 765 496 6105.
E-mail addresses: aziabari@purdue.edu (A. Ziabari), suhire@aol.com (E. Suhir), shakouri@purdue.edu (A. Shakouri).

0026-2692/$ - see front matter © 2013 Elsevier Ltd. All rights reserved.
http://dx.doi.org/10.1016/j.mejo.2013.12.004

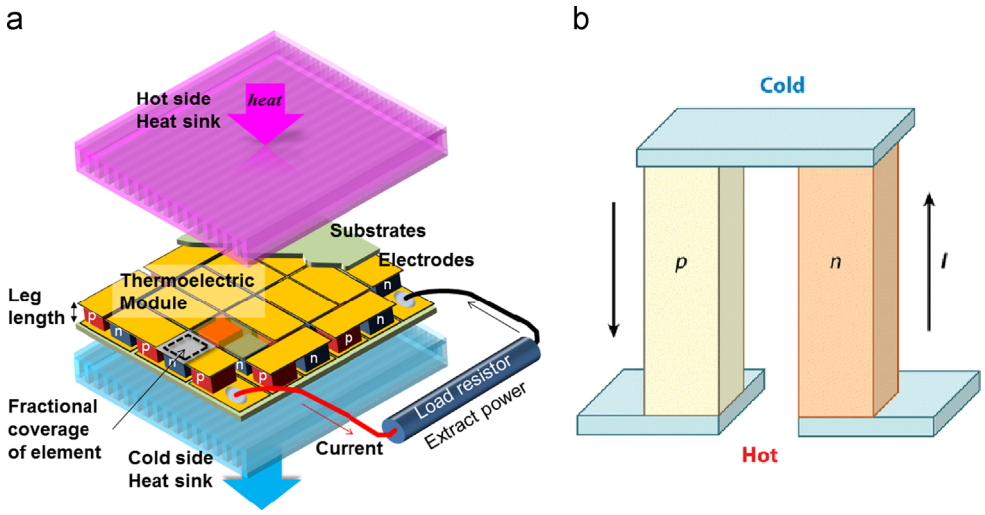

Fig. 1. Thermo-electric module; (a) general view; (b) a two leg module with n-type and p-type legs.

structure idealized as a long-and-narrow strip could be considered.

- The bonded TEM ceramic components can be treated, from the standpoint of structural analysis, as elongated rectangular plates that experience linear elastic deformations, and approximate methods of structural analysis and materials physics can be used to evaluate the induced stresses and displacements.
- The interfacial shearing stresses can be evaluated based on the concept of the interfacial compliance [14].
- The interfacial compliances of the bonded components and the TEM legs can be evaluated, however, based on the Rebière solution in the theory-of-elasticity for a long-and-narrow strip (see, e.g., [14]).
- The assembly is thick and stiff enough, so that it does not experience bending deformations, or, if it does, bending does not affect the interfacial thermal shearing stresses and need not be accounted for.
- The interfacial shearing stresses can be evaluated without considering the effect of "peeling", i.e., the normal interfacial stresses acting in the through-thickness direction of the assembly.
- The longitudinal interfacial displacements of the TEM bonded components can be sought as the sum of (1) the unrestricted stress-free displacements, (2) displacements caused by the thermally induced forces acting in the cross-sections of the TEM components and (3) additional displacements that consider that, because the thermal loading is applied to the component interface, the interfacial displacements are somewhat larger than the displacements of the inner points of the component.
- TEM legs provide mechanical supports for the TEM bonded components (ceramics) and their interfacial compliance is critical when one intents to buffer the interfacial stress, but do not experience thermal loading themselves.

Some additional, more or less minor, assumptions are indicated in the text of the paper.

2.2. Interfacial compliance

Analytical modeling uses the interfacial compliance concept suggested in Refs. [14–16]. The concept enables one to separate the roles of the design (its geometry and material properties) and the loading caused by the change in temperature and/or temperature gradients. The approach is based on and reduced to the evaluation

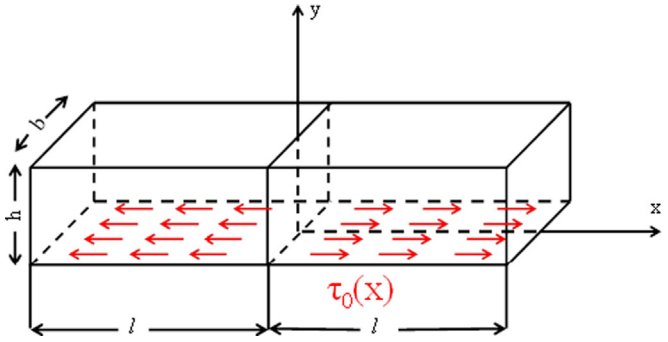

Fig. 2. Elongated strip subjected to shear loading.

of the longitudinal interfacial compliance of a strip subjected to the longitudinal shear loading applied to its long edge (Fig. 2). An important assumption underlying the rationale behind the employed analytical model is that the actual 3D structural element (experiencing in a multi-material body interfacial loading caused by the dissimilar materials in the body) can be substituted by an elongated strip that is, in effect, the longitudinal cross-section of the body. The following approximate formula for the longitudinal displacements of the edge of such a strip has been used [14–16] to evaluate the longitudinal displacements of a strip loaded over its long edge by a distributed shear loading:

$$u_0 = -\frac{1-\nu^2}{Ehb}\int_0^x Q(\xi)d\xi + \kappa\tau_0(x) \quad (1)$$

Here E and ν are the modulus of elasticity and Poisson's ratio for the strip material, κ is the longitudinal compliance of the strip (defined as the ratio of the longitudinal displacement to the loading $\tau_0(x)$, h is the thickness of the strip, b is its width, and $Q(x)$ is the distributed longitudinal force acting at the x cross section of the strip. The first term in Eq. (1) reflects an assumption that the displacement of the strip's edge at the x cross section is uniformly distributed over the cross section. The second term account for the deviation of the actual, non-uniform, distribution of this force: the longitudinal displacements at the strip edge, where the load $\tau_0(x)$ is applied, are somewhat greater than at the inner points of the cross section. The structure of this term reflects an assumption that the correction in question can be calculated as the product of the shearing load $\tau_0(x)$ in the given cross section and the longitudinal compliance of the strip, as well as an assumption that the displacement determined by this term is not affected by

Please cite this article as: A. Ziabari, et al., Minimizing thermally induced interfacial shearing stress in a thermoelectric module with low fractional area coverage, Microelectron. J (2014), http://dx.doi.org/10.1016/j.mejo.2013.12.004

the states of stress and strain in the adjacent cross sections. The detailed rationale behind the formula (1) and the subsequent derivation of the interfacial compliance κ can be found in Refs. [14–16]. The obtained general formula for this compliance is

$$\kappa = \frac{\sum_k \gamma_k M(u_k) sin\alpha_k x}{Eb\sum_k \alpha_k \gamma_k sin\alpha_k x} \tag{2}$$

here the function $M(u_k)$ and the parameters α_k, u_k and γ_k are defined as [14–16]:

$$M(u_k) = \left(\frac{1+\nu}{2}\right)\left[(3-\upsilon-(1+\upsilon)u_k cotanhu_k)\, cotanhu_k + (1+\upsilon)u_k - \left(\frac{2(1-\nu)}{u_k}\right)\right]$$

$$\alpha_k = \frac{k\pi}{2l}, \quad u_k = \alpha_k h = \frac{k\pi h}{2\ l}, \quad \gamma_k = \frac{2}{\alpha_k l}\int_0^l \tau_0(x) sin\alpha_k x dx, k = 1,3,5,7,\ldots \tag{3}$$

Only the odd numbers are used in the formulas (2) and (3), because the strip deformations are symmetric with respect to its mid-cross-section.

The interfacial compliance κ depends on the geometry of the strip (ratio h/l of its height h to half of its length $2l$), elastic constants of its material, and, as shown in Fig. 3, also, slightly, on the shear load $\tau_0(x)$. The latter effect is, however, insignificant in comparison with the effects of the aspect ratio of the strip and the properties of its material and in an approximate analysis could be neglected. The expression (2) can be approximated, in extreme situations, by simplified relationships [14–16] and, in the cases of extreme aspect ratios h/l, leads to the following simple formulas:

$$\kappa = \begin{cases} \frac{h}{3Gb} & \frac{h}{l} < 0.5 \\ \frac{3-\upsilon}{2\pi b G}\frac{l}{} & \frac{h}{l} > 2 \end{cases} \tag{4}$$

here $G = (E/2(1+\nu))$ is the shear modulus of the material.

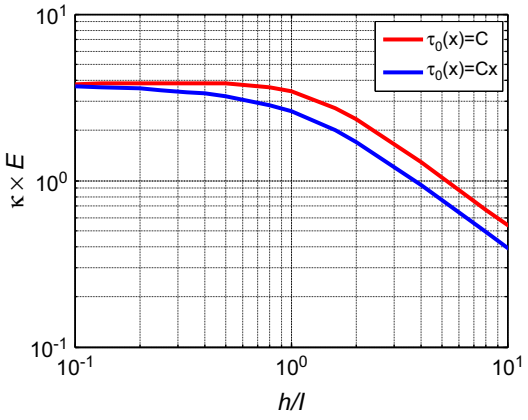

Fig. 3. Evaluation of longitudinal interfacial compliance coefficient for linear shear load distribution (blue curve) as well as uniform shear load distribution (red curve). (For interpretation of the references to color in this figure legend, the reader is referred to the web version of this article.)

The compliance for the intermediate h/l ratios can be obtained, in an approximate analysis, by interpolation. In our further analysis we use, however, the formulas (4) when the h/l ratio is below 0.5 or above 2, and the general formula (2), when the h/l ratio is between 0.5 and 2.0. The κ values computed for different materials employed in the TEM under evaluation (Fig. 4), are based on the assumption that the loading $\tau_0(x)$ is uniformly distributed over the long edge of the strip, i.e., coordinate x independent.

2.3. Shearing stress

As has been indicated above, the analysis is conducted under the major assumption that the bonding systems ("legs") provide mechanical support in the TEM design and their interfacial compliance, in terms of providing a strain buffer between the TEM components is important, but do not experience thermal loading themselves. This assumption seems to be justified in the case of short enough bonds, i.e. in the case of long assemblies with short bonded regions which is the primary situation of interest in this analysis. Such an assumption might result, however, in an overestimation of the induced stresses in the case of not-very-short bonded regions ("not very thin legs"), but could still be supposedly used for the relative assessment of the state of stress in a TEM design in question.

The longitudinal interfacial displacements (Fig. 3) can be predicted using the following approximate formulas:

$$u_1(x) = -\alpha\Delta t_1 x + \lambda_1 \int_0^x T(\zeta)d\zeta - k_1\tau(x); u_2(x) = -\alpha\Delta t_2 x - \lambda_1 \int_0^x T(\zeta)d\zeta + k_1\tau(x) \tag{5}$$

These formulas are similar to those used in [15], where, however, dissimilar bonded component materials were considered. The first terms in Eq. (5) are unrestricted thermal expansions of the TEM components. In these terms, α is the coefficient of thermal expansion (CTE) of the material, Δt_1 and Δt_2 are the change in temperature of the components (from the manufacturing temperature to the operation temperature). The second terms are due to the axial thermally induced forces $T(x) = Q(x)/b$ acting in the cross section of the components. In these terms, $\lambda_1 = (1-\upsilon_1/E_1 h_1)$ is the axial compliance of one of the bonded components, E_1, ν_1, h_1 are the elastic (Young's) modulus, Poisson's ratio of the material and the component thickness, respectively. These terms were evaluated using Hooke's law. The last terms in Eq. (5) account for the actual non-uniform distribution of the forces $T(x)$. These terms reflect an assumption that the corresponding corrections can be evaluated as products of the interfacial compliance and the interfacial shearing stress acting in this cross-section. It is assumed also that these terms are not affected by the states of stress and strain in the adjacent cross-sections.

The condition of the compatibility of the interfacial displacements of the bonded TEM components can be written as

$$u_1(x) = u_2(x) + \kappa_0\tau(x) \tag{6}$$

where κ_0 is the interfacial compliance of the buffering material

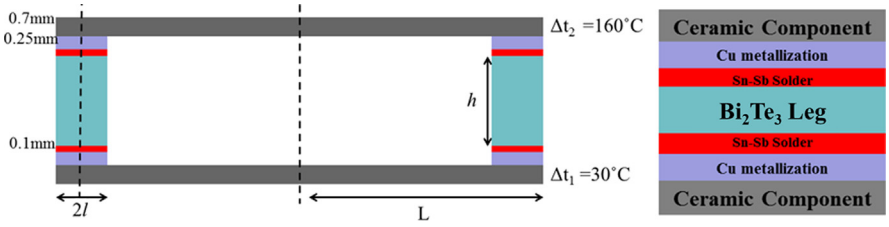

Fig. 4. Thermo-electric module 2D structure. Parameters shown in the figure are used for case studies in Section 3.

(structure). Substituting the displacements (5) into the condition (6), one can obtain a governing equation for the force $T(x)$, and the solution to this equation can be sought in the form:

$$T(x) = \frac{-\alpha\Delta T}{2\lambda_1} + C_1 \sinh kx + C_2 \cosh kx \tag{7}$$

where the first term is the particular solution for the inhomogeneous governing equation and the second and the third terms provide the general solution to the corresponding homogeneous equation. The constants C_1 and C_2 are constants of integration. In Eq. (7)

$$k = \sqrt{\frac{2\lambda_1}{\kappa}} \tag{8}$$

is the parameter of the interfacial shearing stress and κ is the total interfacial compliance of the TEM assembly.

The solution (7) must satisfy the boundary conditions:

$$T(-l) = \hat{T}, \quad T(l) = 0 \tag{9}$$

The compatibility condition for the longitudinal displacements at the bonded and unbonded regions of the TEM assembly can be written as follows:

$$\kappa\tau(-l) = 2\lambda_1 \hat{T}(L - 2l) \tag{10}$$

In these equations, $\hat{T}$ are the forces that determine the role of the global mismatch of the components. Global mismatch occurs outside the bonded region because of the mismatch of assembly components, while local mismatch occurs within the bonded regions and is due to the thermal mismatch of the materials. From (7)–(9) and the obvious relationship $T'(x) = \tau(x)$, one can find the force $\hat{T}$, *and* $T(x)$ acting in the unbonded and bonded regions, respectively, and the interfacial shearing stress. Subsequently, the following expression for the interfacial shearing stress could be obtained:

$$\tau(x) = k\frac{\alpha\Delta T}{2\lambda_1}\left[\frac{\sinh kx}{\cosh kl} + \frac{\tanh kl}{2kl((L/2l)-1)\sinh 2kl + \cosh 2kl}\cosh k(l-x)\right], \quad \frac{L}{2l} \geq 1 \tag{11}$$

A detailed explanation of derivation of these equations could be found in Ref. [12].

The maximum interfacial shearing stress takes place at the assembly edges:

$$\tau(l) = k\frac{\alpha\Delta T}{2\lambda_1}\tanh kl\left[1 + \frac{1}{2kl((L/2l)-1)\sinh 2kl + \cosh 2kl}\right], \frac{L}{2l} \geq 1 \tag{12}$$

This relationship indicates that by decreasing the product kl of the parameter of the interfacial shearing stress and half the length of the bonded region one could reduce the maximum interfacial shearing in this region.

3. Case studies

The analytical solution described in Section 2 is applied to the TEM structure shown in Fig. 4. The material properties are given in Table 1. Three different assembly sizes of 10 mm, 20 mm and 40 mm (L=5 mm, 10 mm, and 20 mm) were chosen. The value of l, the half the bonded region length, has been varied to evaluate its effect on the maximum interfacial shearing stress. The temperature difference between the top and the bottom components (ΔT) is 130 °C. The thickness of the TEM leg is 4 mm. Bonded region and component thicknesses are as indicated in Fig. 4.

The maximum interfacial shearing stress versus bonded region length for different assembly lengths is obtained using the analytical model presented in Section 2. The results are plotted in Fig. 5. As it can be seen, the decrease in the length of the bonded region results in lower maximum interfacial shearing stress. Also, for the same bonded region length, the increase in the assembly's length leads to the decrease in the maximum interfacial shearing stress. This means that the increase in the $L/2l$ ratio and the decrease in the fractional area coverage of the thermoelectric legs lead to lower maximum interfacial shearing stresses.

Table 1
Mechanical properties of materials employed in TEM.

Material	Young modulus (GPa)	CTE (ppm/°C)	Poisson's ratio
Ceramic component	380	6.5	0.28
Copper stripe (metallization)	115	17	0.31
Sn–Sb solder layer	44.5	27	0.33
Be_2Te_3 leg	47	16.8	0.4

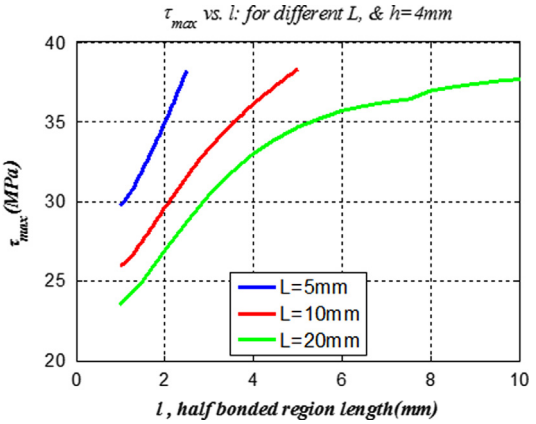

Fig. 5. Variation of maximum interfacial shear stress (τ_{max}) vs bonded region's length for different assembly lengths, $2L$=10 mm (blue), 20 mm (red), and 40 mm (green). (For interpretation of the references to color in this figure legend, the reader is referred to the web version of this article.)

Finite element modeling (FEM) software, ANSYS, has been used to simulate the same TEM assembly. The 8 nodes plane 223 element in plane strain mode were used. The structure is meshed with very fine square elements. Each element is $25 \times 25\ \mu m^2$ and there were around 400,000 elements in this structure. A sample meshed structure is shown in Fig. 6. The boundary conditions of the simulations were set according to the boundary conditions in the analytical model. The strain free temperature (reference temperature) is set to zero. Then the top component heated up to 160 °C and the bottom component is heated up to 30 °C. Temperature load applied to the structure is shown in Fig. 7a. The deformed shape of the TEM structure due to this temperature load is superimposed on the edge of original un-deformed model. The translation is restrained in both x and y direction in the bottom corners of the TEM structure. A vertical cross section of the temperature profile is plotted in Fig. 7b. The material properties are set according to Table 1. The coefficient of thermal expansion (CTE) for the ceramic plates is set to 6.5×10^{-6} (1/°C).

For other layers we consider two cases. In the first case we set the same CTE for them as the components. In the second case we set them to the value shown in Table 1.

The maximum shearing stresses for different assembly lengths and bonded region length sizes are calculated using ANSYS. The results are compared with the analytical solutions in Fig. 8a and b. In Fig. 8a the half assembly length (L) is 5 mm, the leg thickness (h) is 4 mm and half bonded region length (l) is changing 0.5 mm to

Please cite this article as: A. Ziabari, et al., Minimizing thermally induced interfacial shearing stress in a thermoelectric module with low fractional area coverage, Microelectron. J (2014), http://dx.doi.org/10.1016/j.mejo.2013.12.004

2 mm. Also, the same simulations have been done for an assembly with L equal to 10 mm and l changing from 1 mm to 4 mm. It can be seen in both cases that our analytical model follows the same trend as FEM and the results are in good agreement. Changing fractional coverage area by a factor of 16 from 64% to 4% resulted in a maximum 40% drop in the interfacial shear stress in each case. Fig. 9 shows that if we consider CTE mismatch between the layers as well the values for stress would increase significantly for this particular case study. However, this figure is also indicative of the same trend for maximum interfacial shear stress. It can be seen in Fig. 9 that, for the TEM structure used in this case study with the material property listed in Table 1, lowering the fractional coverage area by a factor of 16 from 64% to 4% will lead to about 32% drop in maximum interfacial shear stress, which matches our analytical model.

The decrease in the TEM leg thickness results in higher maximum interfacial shearing stresses. This is shown in Fig. 10. Both ANSYS and the analytical model show similar results as the thermoelectric leg thickness decreases. These simulations are performed for a structure with L and l equal to 5 mm and 2 mm, respectively. Increasing the leg thickness by a factor of 10 leads to a 70% drop in the maximum interfacial shearing stress. As evident from these figures, analytical and numerical data are in good agreement.

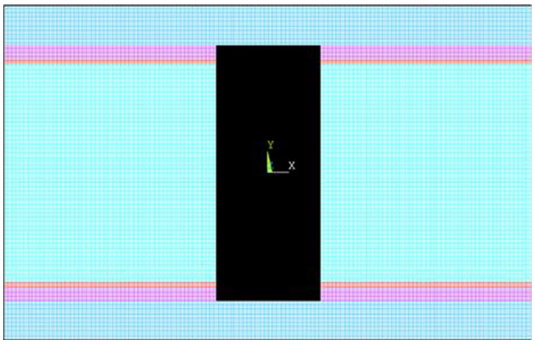

Fig. 6. A sample meshed 2D structure.

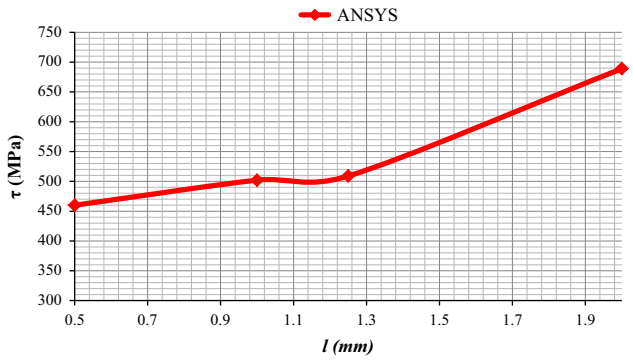

Fig. 9. Maximum interfacial shear stress obtained by ANSYS (red curve) for the TEM structure with right values of CTE (shown in Table 1).

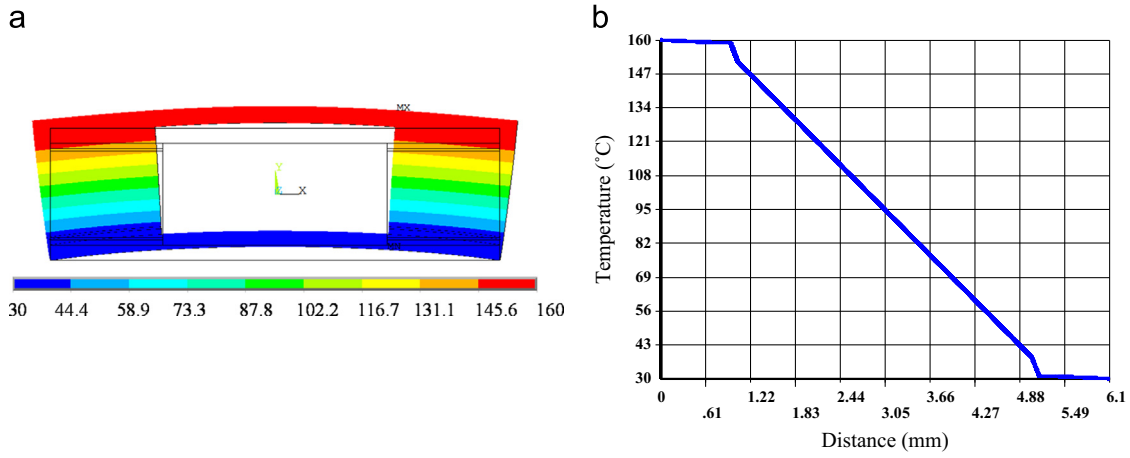

Fig. 7. (a) A sample deformed shape of a 2D TEM simulated in ANSYS is superimposed on the edge of the un-deformed 2D TEM model. (b) Temperature along vertical cross section of one of the legs.

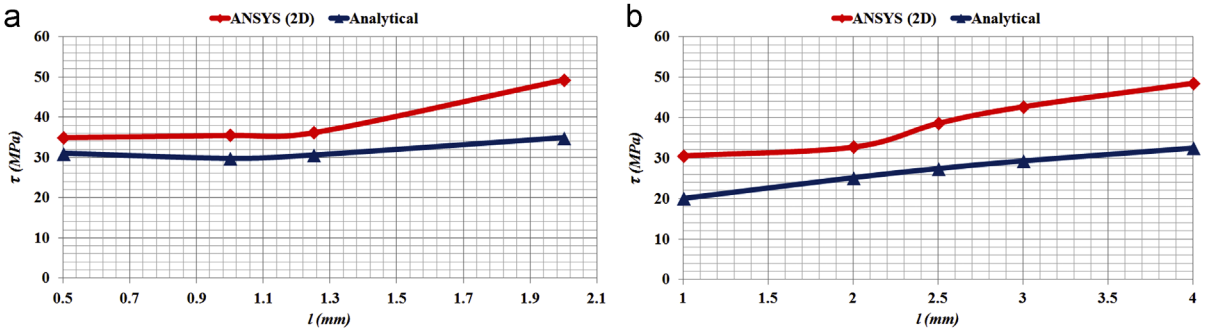

Fig. 8. (a) Maximum interfacial shear stress obtained by ANSYS (red curve) and analytical model (blue curve) for $h=4$ mm and $L=5$ mm. (b) Maximum interfacial shear stress obtained by ANSYS (red curve) and analytical model (blue curve) for $h=4$ mm and $L=10$ mm. (For interpretation of the references to color in this figure legend, the reader is referred to the web version of this article.)

Please cite this article as: A. Ziabari, et al., Minimizing thermally induced interfacial shearing stress in a thermoelectric module with low fractional area coverage, Microelectron. J (2014), http://dx.doi.org/10.1016/j.mejo.2013.12.004

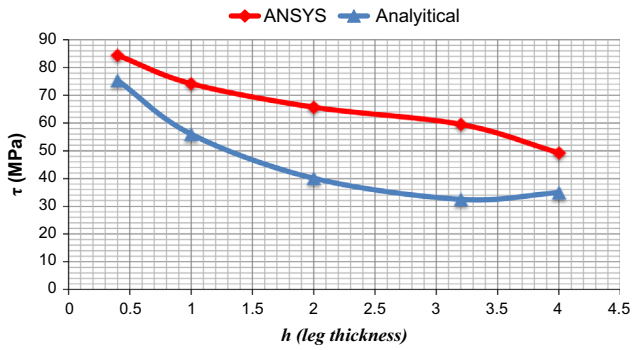

Fig. 10. Maximum interfacial shear stress obtained by ANSYS (red curve) and analytical model (blue curve) for $L=5$ mm and $l=2$ mm, while h changing from 0.4 mm to 4 m. (For interpretation of the references to color in this figure legend, the reader is referred to the web version of this article.)

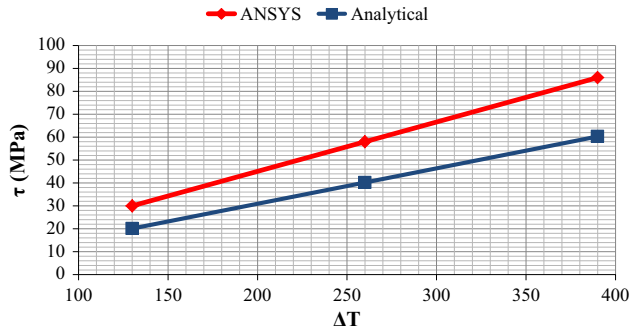

Fig. 11. Maximum interfacial shear stress vs. top and bottom components temperature difference obtained by ANSYS (red curve) and Analytical model (blue curve) for $L=10$ mm and $l=1$ mm, and $h=4$ m. (For interpretation of the references to color in this figure legend, the reader is referred to the web version of this article.)

It is indicated in Fig. 5. that by decreasing the bonded region length the maximum shear stress decreases. On the other hand, by decreasing the TE leg thickness, the maximum shear stress would increase. Therefore, employment of thinner and longer legs could indeed result in a substantial stress relief, thereby leading to a more mechanically robust TEM. In [9] a similar conclusion was achieved with 3D simulation of a 2 leg thermoelectric module.

Eq. (12) shows that, based on our analytical model, the maximum interfacial shear stress varies linearly with the temperature difference between the top and bottom ceramic components. Three simulations are performed in ANSYS with ΔT equal to 130 °C, 260 °C, and 390 °C. For these simulations we chose a 2D structure with L, l, and h equal to 10 mm, 1 mm, and 4 mm, respectively. The results are plotted in Fig. 11. As it can be seen in the figure, increasing of the temperature difference between the components by a factor of 2 and 3 will result in a factor of 2 and 3 augmentations in the value of maximum shear stress in both the analytical model and ANSYS results.

3D simulation is also carried out to confirm what was obtained analytically. The meshed structure is shown in Fig. 12. Symmetry is used and a quarter of the model is simulated. Again, the simulations are performed for two half assembly lengths (L) of 5 mm and 10 mm. The TE leg thickness is chosen to be 4 mm. The temperature difference between the ceramic components is set to 130 °C. By changing the bonded region length, the fractional coverage area in both cases is reduced from 64% to 4%. As can be observed in Fig. 13, 3D simulation shows that the maximum shear stress reduces by a maximum 80%. A comparison between the results of 2D ANSYS simulation, analytical model, and 3D ANSYS simulation for both case studies is shown in Fig. 13. The analytical solution has occurred between the two FEA solutions and follows the same trend. Intuitively this behavior seems reasonable, as the analytical model indirectly, by bringing in the Young's modulus and the Poisson's ratio, takes into account (in an approximate

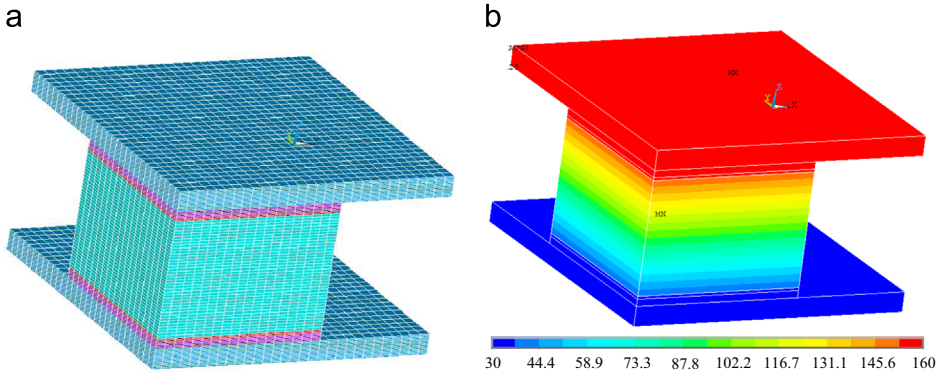

Fig. 12. (a) 3D meshed structure. (b) Temperature profile.

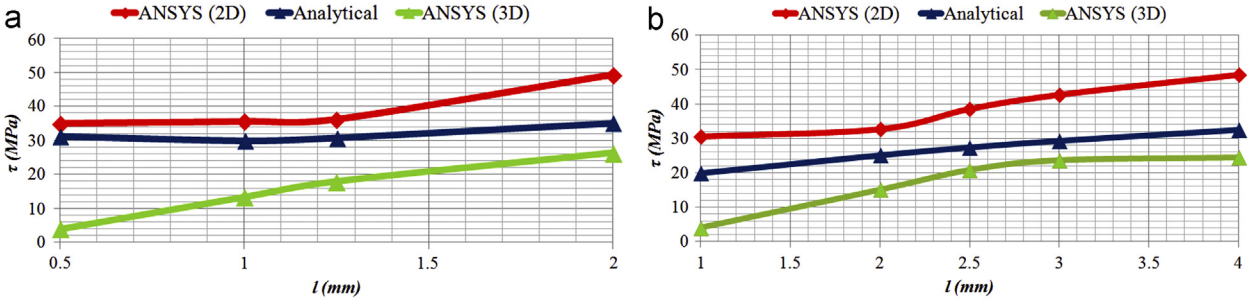

Fig. 13. Comparison between Analytical results with 3D and 2D ANSYS results. Maximum shear stress vs. half bonded length is plotted for (a) $L=5$ mm, $h=4$ mm. (b) $L=10$ mm, $h=4$ mm.

Please cite this article as: A. Ziabari, et al., Minimizing thermally induced interfacial shearing stress in a thermoelectric module with low fractional area coverage, Microelectron. J (2014), http://dx.doi.org/10.1016/j.mejo.2013.12.004

fashion) the 3D state of stress. The difference between the maximum shear stress values, obtained by analytical model in comparison with ANSYS 2D and 3D results, is due to the fact that the analytical model is neither a 3D nor an exactly 2D model. The reason is the geometry of TEMs is complex and cannot be considered as a plane strain or plane stress problem. Our Quasi-2D analytical model takes the Poisson′s ratio into account (in an approximate fashion), while in ANSYS and other FEM a plain strain or plane stress condition for 2D problem needs to be defined.

4. Conclusion

The longitudinal interfacial compliance for the uniform and linearly distributed shear loading along the interface of a long-and-narrow strip has been evaluated in application to assemblies of the TEM type. The evaluated compliances were employed, using analytical modeling, to calculate the maximum shear stress in a TEM design with two legs at the ends. Finite element 2D and 3D simulations in ANSYS were carried out to verify the results obtained by the analytical model. Different comparisons are conducted and it is demonstrated that the simple analytical model presented in this work is in good agreement with the results obtained by the finite element method. It is shown that the maximum interfacial thermally induced shearing stress occurs at the leg′s corner and employment of thinner and longer legs could indeed result in a substantial stress relief. Some case studies are presented as a proof of concept. It is shown that by thinning the leg length by a factor of four, and in turn, decreasing the fractional area by a factor of 16, maximum shear stress dropped by 80%. It should be pointed out that the presented analytical model captures the trends very well in comparison with 2D and 3D finite element results, even though the values are quite different. The difference comes from the complex geometry of the structure and because it cannot be considered as an exact 2D plane stress or plane strain problem. One of the main characteristics of an analytical model is that it should be able to distinguish between different parameters and illustrates how variation of each of them would affect the final value of the results. To that end, the significance of this analytical model over FEM is that it can be utilized to clarify the effect of different parameters in the model without the need for expensive computation. Authors believe that the numerical examples of this paper will guide someone skilled in the field to design the most mechanically feasible TEM structure.

References

[1] A. Shakouri, Recent developments in semiconductor thermoelectric physics and materials, Annu. Rev. Mater. Sci. 41 (2011) 399–431.
[2] K. Fukutani, A. Shakouri, Design of bulk thermoelectric modules for integrated circuit thermal management, IEEE Trans. Compon. Packag. Technol. 29 (4) (2006) 750–757.
[3] X. Fan, G. Zhang, C. Labounty, D. Vashaee, J. Christopherson, A. Shakouri, J. E. Bowers, Integrated cooling for Si-based microelectronics, in: Proceeding IEEE International Conference on Thermoelectric, 2001, pp. 405–408.
[4] A. Shakouri, Y. Zhang, On-chip solid-state cooling for integrated circuits using thin-film microrefrigerators, IEEE Trans. Compon. Packag. Technol. 28 (1) (2005) 65–69.
[5] I. Chowdhury, R. Prasher, K. Lofgreen, G. Chrysler, S. Narasimhan, R. Mahajan, D. Koester, R. Alley, R. Venkatasubramanian, On-chip cooling by superlattice-based thinFilm thermoelectrics, Nat. Nanotechnol. 4 (2009) 235–238. (April).
[6] K. Takahata, Micro Electronic and Mechanical Systems, InTech, December 01, 2009 Under CC BY-NC-SA 3.0 License.
[7] J-H. Bahk, R.B. Sadeghian, Z. Bian, A. Shakouri, Seeback enhancement through miniband conduction in III–V semiconductor superlattices at low temperatures, J. Electron. Mater. (2012). (Published online Feb.8).
[8] G. Joshi, et al., Enhanced thermoelectric figure-of-merit in nanostructured p-type silicon germanium bulk alloys, Nano Lett. 8 (12) (2008) 4670–4674.
[9] J. Bierschenk, M. Gilley, Assesment of TEC thermal and reliability requirements for thermoelectrically enhanced heat sinks for CPU cooling applications, in: 2006 International Conference on Thermoelectrics (ICT), 2006, pp. 254–259.
[10] T. Clin, S. Turenne, D. Vasilevskiy, R.A. Masut, Numerical simulation of the thermomechanical behavior of extruded bismuth relluride alloy module, J. Electron. Mater. 38 (7) (2009) 994–1001.
[11] J.L. Gao, Q.G. Du, X.D. Zhang, X.Q. Jiang, Thermal stress analysis and structure parameter selection for a Bi_2Te_3 based thermoelectric module, J. Electron. Mater. 40 (5) (2011) 884–888.
[12] E. Suhir, A. Shakouri, Assembly bonded at the ends: could thinner and longer legs result in a lower thermal stress in a thermoelectric module design? J. Appl. Mech. 79 (2012) 061010.1–061010.8. (Nov.).
[13] ANSYS 14., 2012 ANSYS, Inc.
[14] E Suhir, Structural Analysis in Microelectronics and Fiber Optics, Van-Nostrand, New York, 1973.
[15] E. Suhir, Stresses in bi-metal thermostats, Trans. ASME J. Appl. Mech. 53 (3) (1986) 657–660.
[16] E. Suhir, Stresses in adhesively bonded bi material assemblies used in electronic packaging, in, Proceedings of the Electronic Packaging Material Science-II, MRS Symposium, 1986, 133–138.

Please cite this article as: A. Ziabari, et al., Minimizing thermally induced interfacial shearing stress in a thermoelectric module with low fractional area coverage, Microelectron. J (2014), http://dx.doi.org/10.1016/j.mejo.2013.12.004